THE JOURNAL OF BIOLOGICAL CHEMISTRY
Vol. 267, No. 16, Issue of June 5, pp. 11289-11299, 1992
Printed in U.S.A.

Effects of the Neuronal Phosphoprotein Synapsin I on Actin Polymerization

II. ANALYTICAL INTERPRETATION OF KINETIC CURVES*

(Received for publication, August 15, 1991)

Riccardo Fesce‡, Fabio Benfenati§, Paul Greengard¶, and Flavia Valtorta‡‖

From the ‡"Bruno Ceccarelli" Center for the Study of Peripheral Neuropathies, Department of Medical Pharmacology, National Research Council Center of Cytopharmacology, San Raffaele Scientific Institute, University of Milano, 20129 Milano, Italy, the §Institute of Human Physiology, University of Modena, 41100 Modena, Italy, and the ¶Laboratory of Molecular and Cellular Neuroscience, The Rockefeller University, New York, New York 10021-6399

The general features of the kinetics of actin polymerization are investigated by mathematical models, with the aim of identifying the kinetically relevant parameters in the process and detecting and interpreting the alterations occurring in actin polymerization under various experimental conditions. Polymerization curves, obtained by following the increase in fluorescence of actin derivatized with *N*-(1-pyrenyl) iodoacetamide, are fitted using analytical equations derived from biochemical models of the actin polymerization process. Particular attention is given to the evaluation of the effects of the neuronal phosphoprotein synapsin I. The models obtained under various ionic conditions reveal that synapsin I interacts with actin in a very complex fashion, sharing some of the properties of classical nucleating proteins but displaying also actions not described previously for other actin-binding proteins. Synapsin I appears to bind G-actin with a very high stoichiometry (1:2–4), and the complex behaves as an F-actin nucleus, producing actin filaments under conditions where spontaneous polymerization is negligible. These actions of synapsin I are markedly affected by site-specific phosphorylation of the protein. An original transformation of the fluorescence data, which estimates the disappearance rate of actin monomer toward the critical concentration, is presented and shown to be of general usefulness for the study of actin-binding proteins.

Actin polymerization is a cooperative process involving the sequential condensation of actin monomers. When a critical size is reached the complex is generally referred to as a "nucleus" and its growth becomes favored (Oosawa and Asakura, 1975; Wegner, 1976; Wegner and Engel, 1975). Two phases can be distinguished in the polymerization process: (i) nucleation, *i.e.* complexing of monomers to constitute oligomeric intermediates below the critical size and (ii) elongation of the filaments (or simply "polymerization") which occurs as long as the concentration of monomers is sufficiently high to sustain the sequential addition of monomers to the filaments. Polymerization "stops" when the monomer concentration falls to a level where addition and loss of monomers reach equilibrium. This concentration is generally referred to as the critical concentration (CC),[1] since no detectable polymerization of actin is expected to occur below such a concentration, whereas generation and elongation of filaments are expected at higher monomer concentrations.

The nucleation process implies a sequence of reactions among monomers and unstable oligomers, possibly with different rate constants for the various reactions and forms of G-actin (Ca^{2+}/Mg^{2+}-, ATP/ADP-actin). The elongation process appears to involve filament-monomer interactions at the two ends of the filament, which are not equivalent: addition of monomers is favored at the "barbed end," whereas at the "pointed end" monomer dissociation preferentially occurs (for reviews see Korn, 1982; Frieden, 1985; Pollard and Cooper, 1986, Gaertner *et al.*, 1989; Carlier, 1991). Thus, the nucleation/elongation process involves many biochemical parameters, and its modeling requires a very complex system of differential equations, giving rise to an intractable mathematical problem.

A small series of operational parameters can be devised to simplify the mathematical modeling (see Wegner and Engel, 1975; Cooper *et al.*, 1983a; Tobacman and Korn, 1983). If a nucleus is constituted by n monomers, a close approximation to the kinetics of nucleation is provided by stating that the number of nuclei generated per unit of time is proportional to the nth power of monomer concentration. The proportionality factor is an operational quantity related to a combination of the forward and backward rate constants for the addition of the first n monomers and can be considered as a "nucleation rate constant." In a similar manner, a single overall rate constant for elongation (equal to the sum of the rate constants for the barbed and pointed ends) can be considered, as well as a single affinity constant (*i.e.* the combined affinity of the two ends of the filaments, which equals CC).

Simplified kinetic models of actin polymerization under various experimental conditions have been proposed, using such operational quantities. The curves fitting the time

* This work was supported by Consiglio Nazionale delle Ricerche Progetto Strategico "Meccanismi di Release dei Neurotrasmettitori e loro Controllo" (to F. B.), Progetto Speciale "Meccanismi Molecolari di Trasduzione del Segnale" (to F. V.), and Progetto Finalizzato "Invecchiamento" (921132), NATO Collaborative Grant 0039/89 (to F. B. and P. G.), and by United States Public Health Service Grant MH 39327 (to P. G.). The support of Telethon (to F. V., F. B., and R. F.) is also acknowledged. The costs of publication of this article were defrayed in part by the payment of page charges. This article must therefore be hereby marked "*advertisement*" in accordance with 18 U.S.C. Section 1734 solely to indicate this fact.

‖ To whom correspondence should be sent: "B. Ceccarelli" Center, Dept. of Medical Pharmacology, University of Milano, Via Vanvitelli 32, I-20129 Milano, Italy. Tel.: 39-276110224; Fax: 39-27490937.

[1] The abbreviations used are: CC, critical concentration; G-actin, globular actin; F-actin, filamentous actin; AMBR, actin monomer binding rate; CaM kinase II, Ca^{2+}/calmodulin-dependent protein kinase II; EGTA, [ethylenebis(oxyethylenenitrilo)]tetraacetic acid; LIS, low ionic strength; HIS, high ionic strength.

courses of polymerization were obtained from the corresponding differential equations by means of trial-and-error search for the parameters and iterative numerical integration (*e.g.* Tobacman and Korn, 1983; Frieden, 1983; Cooper *et al.* 1983a; Cooper and Pollard, 1985). Actin polymerization can be monitored in the spectrofluorometer by measuring the fluorescence of a mixture of native and pyrene-conjugated actin, as pyrene increases its quantum yield when actin polymerization exposes it to a hydrophobic environment, and the increase in fluorescence intensity from its initial value is proportional to the quantity of filamentous actin (Kouyama and Mihashi, 1981; Cooper *et al.*, 1983b), although the linearity of the relation is not perfect (Grazi, 1985).

In this study we derive the analytical functions corresponding to the differential equations of the simplified polymerization model. This allows to fit curves by standard methods of minimization of the square errors and to detect and interpret the departures from typical behavior observed under various experimental conditions. Particular attention has been paid to the effects of synapsin I on the kinetics of actin polymerization. As illustrated in the accompanying paper (Valtorta *et al.*, 1992), the time course of actin polymerization is markedly altered by synapsin I. The analytical description of the normal process of actin polymerization makes it possible to recognize the specific changes in the kinetics of the system brought about by the interaction of synapsin I with actin.

An original transformation of the raw fluorescence data is also presented, which appears to be particularly useful in studying the actions of proteins and drugs in the nucleation phase and in discriminating the effects displayed by actin-binding proteins on nucleation rather than on polymerization.

EXPERIMENTAL PROCEDURES

Methods

Experimental procedures were those described in Valtorta *et al.* (1992). Freshly purified G-actin in buffer A (0.2 mM $CaCl_2$, 0.2 mM ATP, 0.5 mM NaN_3, 0.5 mM β-mercaptoethanol, 2 mM Tris-HCl, pH 8.0) was kept on ice under continuous dialysis against the same buffer and used within 2–3 days. Polymerization was triggered by the addition of 30 mM KCl and 1 mM $MgCl_2$ at time 0, unless otherwise stated. Either 15 mM NaCl (low ionic strength, LIS) or 85 mM NaCl (high ionic strength, HIS) was added before polymerization was started. Digitized curves (one reading/2 s) of pyrenyl-actin fluorescence were transferred to a M-211V personal computer (Olivetti, Italy) for data processing. All curve fittings were performed by iterative search of the best fitting parameters according to standard procedures of minimization of the square residuals ("least squares fit"). All mathematical processing was performed using PC-MATLAB software (Rapid Data Inc., United Kingdom). Curves reproduced from papers by other authors (see Fig. 8) were manually digitized on enlarged photocopies of the original figures using a graphic tablet connected to an Apple computer and then transferred to the Olivetti computer for processing.

Theory

Several extensive investigations and review papers have been published concerning the molecular mechanisms of nucleation and elongation of actin filaments, and the effects of ionic strength, divalent cations, and adenosine nucleotides on these processes (Frieden, 1985; Korn, 1982; Tobacman and Korn, 1983; Carlier, 1991). In this study we have focused our attention on the kinetic aspects of actin polymerization and have produced a mathematical model based on the above-mentioned systematic analyses which allows one to predict and interpret changes in the kinetics induced by interference with the various steps of the process.

Elongation of Actin Filaments—The number of actin monomers added to pre-existing filaments per unit time is proportional to the number of filaments, the concentration of monomeric actin, and the sum of the association rate constants at the pointed and barbed ends of the filament (twice the mean rate constant, in general, if various forms of monomers, with different reactivities due to binding with divalent cations and adenosine nucleotides, are considered). The number of actin monomers released by the filaments per unit time is proportional to the number of filaments and to the sum of the dissociation rate constants at the two ends of the filament (twice the mean dissociation rate constant, in general). The sum of the association rate constants can be replaced by a single operational factor, the "combined association rate constant," K^+, and the analogous factor K^- can replace the two dissociation rate constants, yielding Scheme I, where F_l indicates a filament composed by l monomers and A is G-actin. Equilibrium is reached for actin monomer concentration $CC = K^-/K^+$ and the loss of actin monomers due to filament elongation is described as follows,

$$(d/dt)\ A = -K^+ \cdot F \cdot A + K^- \cdot F = -K^+ \cdot F \cdot (A - CC) \qquad (1)$$

where A = G-actin concentration, F = actin filament concentration, and K^+ ($M^{-1}\ s^{-1}$), K^- (s^{-1}), and CC (M) have been defined above.

Since the loss of monomers due to nucleation is likely to be significant only in the very beginning of the reaction, Equation 1 describes the changes in G-actin concentration over most of the time course of actin polymerization. The following are from Equation 1:

$$(d/dt)\ (A - CC) = -K^+ \cdot F \cdot (A - CC) \qquad (1a)$$

$$(d/dt)\ \log(A - CC) = -K^+ \cdot F \qquad (1b)$$

Equation 1a is Equation 1 from Tobacman and Korn (1983). Equation 1b states that the time derivative of the logarithm of actin concentration in excess of CC (*i.e.* the fractional reduction of the G-actin concentration per unit of time or excess monomer disappearance rate) directly monitors the concentration of filaments and nuclei and therefore is very useful in analyzing polymerization in the presence of preformed nuclei or nucleating proteins (see below).

Nucleation—The nucleation process involves a series of reactions of monomer addition to mono/oligomers up to the order of the "nucleus" (n). This system is likely to be kinetically complex, with different rate constants for the various steps in the sequence of reactions (Oosawa and Asakura, 1975; Wegner and Engel, 1975; Wegner, 1976). The number of different rate constants may further increase due to the possible coexistence of Mg^{2+}/G-actin, Ca^{2+}/G-actin and ADP- or ATP-associated G-actin (Frieden, 1985; Carlier, 1991). Such a system may be simplified according to Scheme II, where A_j indicates oligomers or polymers of jth order. The system is treated analytically in Appendix I, where we show that the number (or concentration) of new nuclei formed per unit time, $(d/dt)\ F$, is proportional to the nth power of the G-actin concentration, A_n, although a delay is expected between the time courses of A_n and $(d/dt)\ F$. The delay is likely to be significant under conditions where the rate constants are high (*i.e.* polymerization is fast), as is the case in Ca^{2+}-free solutions (Appendix I). Neglecting the delay, the system can be reduced as shown in Scheme III, where, in principle, the equilibrium concentration of monomers for nucleation is determined by K_n and may be different from the critical concentration for elongation (CC); however, nuclei are subtracted by the elongation

$$F_l + A \underset{K^-}{\overset{K^+}{\rightleftharpoons}} F_{l+1}$$

SCHEME I

$$\begin{cases} A_1 + A_1 \underset{\beta_1}{\overset{\alpha_1}{\rightleftharpoons}} A_2 \ldots . A_j + A_1 \underset{\beta_j}{\overset{\alpha_j}{\rightleftharpoons}} A_{j+1} & \text{for } j < n \\ A_j + A_1 \underset{K^-}{\overset{K^+}{\rightleftharpoons}} A_{j+1} & \text{for } j \geq n \end{cases}$$

SCHEME II

$$\begin{cases} A^n \overset{K_n}{\leftrightarrow} A_n \\ A_n + A_1 \underset{K^-}{\overset{K^+}{\rightleftharpoons}} A_{n+1} \end{cases}$$

SCHEME III

process above CC, whereas they accumulate and dissociate at CC, so that nucleation occurs as long as the monomer concentration is above CC.[2] Thus, nucleation is closely modeled by Equation 2,

$$(d/dt)\ F = K_n \cdot (A - CC)^n \quad (2)$$

where K_n ($M^{-(n-1)}\ s^{-1}$) is an operational quantity which can be called the nucleation rate constant.

Combining Equations 1b and 2, and introducing the quantity $X = (A - CC)$, "excess" G-actin concentration, the following relation is obtained.

$$(d^2/dt^2)\ \log X = -K^+ \cdot K_n \cdot X^n \quad (3)$$

Note that: (i) $X(t)$ is a quantity directly measurable from fluorescence data, as it parallels the difference between the asymptotic concentration of F-actin (asymptotic fluorescence) and the F-actin concentration (fluorescence) at time = t; (ii) the equation can be fitted directly to the fluorescence data (arbitrary units) by simply introducing the multiplier S^{-n} at the right-hand side, where S is the fluorescence scale for F-actin (=[asymptotic fluorescence − initial fluorescence]/[initial G-actin concentration − CC], fluorescence units·M^{-1}); (iii) the equation has the following general analytical solution,

$$X = [C_1 \cdot \cosh(pt + \tau)]^{-2/n} \quad (4)$$

where C_1 and τ are constants.

The Actin Monomer Binding Rate or Excess G-actin Disappearance Rate—In discussing Equation 1 it was pointed out that the function $-(d/dt)\log X$ monitors the number of filaments or nuclei. When actin polymerization is started by adding salts to the solution containing G-actin, the nuclei are initially absent and they gradually start to build up; thus, $-(d/dt)\log X$ starts from zero and increases until nucleation becomes negligible with respect to filament elongation. The asymptotic value of $-(d/dt)\log X$ is proportional to the apparent equilibrium concentration of actin filaments (F_∞) and in particular it equals $K^+ \cdot F_\infty$. If actin filaments or nuclei are added, $-(d/dt)\log X$ starts from a value > 0 and monotonically increases to reach its apparent equilibrium value. If proteins that bind G-actin or "prenuclei" are present, then $-(d/dt)\log X$ may not start from zero and may either increase or decrease, depending on whether the protein-actin complex strictly behaves as a nucleus, favors the formation of nuclei, or forms aggregates with actin monomers which do not further elongate. Note that under these conditions Equations 2–4 will not generally hold.

From these considerations it appears that useful information on the changes introduced in actin polymerization kinetics arise from the $-(d/dt)\log X$ function. This function represents the disappearance rate of the excess monomer and can be referred to as the actin monomer binding rate (AMBR) to indicate that this quantity involves not only filament concentration and elongation rate constant, but also the concentration of exogenous F-actin seeds, nucleating proteins, or G-actin-binding proteins and their respective rate constants for G-actin binding.

In order to compute the disappearance rate, the asymptotic fluorescence must be known. If the experiment is interrupted before fluorometric data reach a plateau, the asymptotic fluorescence can be estimated by a logasymptotic fit of the final part of the curves, when nucleation has become negligible so that G-actin concentration and fluorescence, $Fl(t)$, are expected to relax exponentially to their respective equilibrium values. The asymptotic fluorescence, $Fl(\infty)$, was computed by autoregressive extrapolation, *i.e.* the equation $Fl(t) - Fl(\infty) = [Fl(t-1) - Fl(\infty)] \cdot \alpha$ was solved for α and $Fl(\infty)$ by least-square-error fit.[3] When raw data were used, before computing the actin monomer disappearance rate they were smoothed by interpolating 1 out of 24 original data points (using a standard "spline" routine). When actin polymerization was followed to completion (3–4 h), the plateau values observed in the absence and presence of synapsin I were not markedly different and were totally consistent with those determined by logasymptotic extrapolations performed on the fluorescence data obtained during the first hour of recording. This was not the case in experiments with synapsin I in the absence of nucleating salts; under this condition polymerization curves rapidly approached an apparent equilibrium and were monitored and fitted over this period only (about 20 min). Pelleting data obtained at later times indicate that polymerization kept proceeding, although at a much slower rate, during the following hours (Valtorta *et al.*, 1992).

Fitting Polymerization Curves—The particular case of Equation 4, where the disappearance rate of excess monomer, $R(t) = -(d/dt)\log X = 0$ for time $t = 0$ is as follows.

$$X = X_0 \cdot [\cosh(pt)]^{-2/n} \quad (5)$$

This equation, corresponding to fluorescence = $S \cdot (X_0 - X)$, was used to fit control actin polymerization curves. Equation 5 implies the following.

$$R(t) = -(d/dt)\log X = (2 \cdot p/n) \cdot \tanh(pt) = K^+ \cdot F \quad (6)$$

$$F(\infty) = 2 \cdot p/(n \cdot K^+),\ \textit{i.e.}\ p = (n/2) \cdot R(\infty), \quad (7)$$

and

$$K^+ \cdot K_n = 2 \cdot p^2 \cdot X_0^{-n}/n,\ \textit{i.e.}$$

$$p = (A_0 - CC)^{-n/2} \cdot \sqrt{(n \cdot K^+ \cdot K_n/2)} \quad (7a)$$

Thus:

$$p = K_n \cdot (A_0 - CC)^n / F_\infty = (d/dt)R(0)/R(\infty) \quad (7b)$$

The parameter p has the dimension of a rate constant (s^{-1}), and is proportional to the final disappearance rate, $R(\infty)$ (Equation 7). Furthermore, the rate constant p is determined by the initial excess concentration of G-actin and the nucleation and elongation rate constants (Equation 7a). Note that Equation 7b states that p is the only significant rate constant of the process, and in particular it is the initial rate constant of the rise in the number of filaments (and of R). The relevant biochemical parameters that can be estimated are $K^+ \cdot K_n$ = compound nucleation rate constant ($M^{-n} \cdot s^{-2}$) and $K^+ \cdot F$ = asymptotic disappearance rate of excess monomer (s^{-1}). Either the CC or the fluorescence scale must be determined by other procedures (fluorometrically or by pelleting), as only the fluorescence corresponding to the initial monomer excess ($X_0 = A_0 - CC$) is involved in the model. This problem is bypassed when $CC << A_0$ and X_0 can be approximated to A_0.

The solution for this system, when the monomer disappearance rate is greater than zero since the beginning (F-actin seeds present), is as follows.

$$X = X_0 \cdot \{\cosh[p(t + \tau)]/\cosh(p\tau)\}^{-2/n} \quad (8)$$

Equation (8) was used to fit polymerization in the presence of F-actin seeds.

The situation with synapsin I was clearly more complex. In the absence of K^+/Mg^{2+} (negligible spontaneous nucleation) the disappearance rate was monotonically decreasing with time, whereas in the presence of "nucleating" concentrations of K^+ and Mg^{2+}, it was clearly biphasic (see "Results"), displaying an initial decline followed by a late increase.

Two simplified schemes can be envisioned for proteins that affect nucleation: Scheme IVa, where the nucleation constant K_n has been changed by the nucleating protein to K_n'; and Scheme IVb, where S is the actin binding site on the protein, P (possibly more than 1, say m, provided binding is noncooperative) and PA_m behaves as a nucleus or filament (note that in this case P itself may behave as a nucleus if $m = 1$). Although Scheme IVa predicts a monotonically increasing

$$A^n \overset{K_n'}{\leftrightarrow} A_n$$

SCHEME IVa

$$S + A \overset{K}{\leftrightarrow} SA$$

SCHEME IVb

[2] This implies that nucleation and polymerization will be negligible below the critical concentration. Nevertheless, conditions might exist where nucleation does not occur and where, above CC, polymerization (elongation) might in principle proceed, provided that filaments are already present.

[3] This is the most robust approach, even when the curves reach a plateau and/or the true equilibrium is different from the plateau, due to late changes in the system. In fact, autoregressive fitting estimates the asymptotic value toward which the system is relaxing, at the particular time considered. Thus, the momentary rate constant of actin monomer disappearance would be correctly estimated even though at the end of the available fluorescence recording, changes took place in the system's equilibrium value (*e.g.* by some late rearrangement of filaments).

disappearance rate, Scheme IVb may give rise either to monotonically increasing or to initially declining disappearance rate, depending on whether the complex PA is considered as G-actin or F-actin and in particular, for fluorometric monitoring, on whether the pyrene group increases its fluorescence in the complex PA_j. (Note that defining PA as a "complex," "pseudo-nucleus," or "pseudo-filament" may become arbitrary). The observed decline in disappearance rate suggests that synapsin I may initially bind/nucleate G-actin, with saturable binding capacity, and that the late increase in disappearance rate may be due to the occurrence of spontaneous nucleation, concurrent with the decline in the "synapsin I-driven" polymerization. The biochemical model for such a system is described in Appendix II; for the sake of simplicity, saturated complexes are not further considered in the model. This would imply that they might bind to existing filaments or to each other giving rise to a negligible number of free ends of their own. If most of the complexes gave rise to independent filaments, then the fitting would overestimate the rate constant for spontaneous nucleation, K_n.[4]

The following analytical approximation is derived (Appendix II),

$$X = X_0 \cdot (f/\cosh(g))^{2/n} \quad (9)$$

where f is the analytical function describing saturable receptor/ligand binding kinetics, *i.e.* $f(t) = a/[1 - (1 - a)\cdot e^{-ct}]$. In this function the fractional ligand excess is $a = f(\infty)$, and the rate constant for the process is $c = L_0 \cdot a \cdot k$ (s^{-1}), where L_0 = initial ligand concentration and k = receptor/ligand association rate constant (M^{-1} s^{-1}). For Equation 9, $L_0 = (A_0 - CC)^{n/2}$ and the pool of G-actin undergoing spontaneous polymerization ("synapsin I-independent pool") is $(A_0 - CC)\cdot a^{2/n}$; and g equals the time integral of $f(t)$, multiplied by $p/f(\infty)$ *i.e.*, $g = p\cdot[t - \log(f)/c]$; p is a rate constant with the same meaning as above and determines the final disappearance rate in combination with the nucleation order n (Equation 7). Together with the synapsin I-independent pool, p determines the compound nucleation rate constant $(K^+\cdot K_n)$ according to Equation 7a, with $(A_0 - CC)^n\cdot a^2$ substituting for $(A_0 - CC)^n$.

Equation 9 was used to fit polymerization curves obtained in the presence of synapsin I. In fitting these curves, the order of nucleation (n) was constrained to the value fitted without synapsin I (4); for curves with 300 nM synapsin I, where fluorescence was still markedly increasing at the end of the monitoring period, the asymptotic fluorescence was constrained to the values obtained without synapsin I or with lower concentrations of synapsin I, where a plateau was reached (see above and Valtorta *et al.*, 1992).

RESULTS AND DISCUSSION

Normal Polymerization of G-actin—Fluorometric curves obtained by monitoring the polymerization of G-actin after addition of the appropriate salts (30 mM KCl, 1 mM $MgCl_2$) were quite well fitted by analytical curves described by Equation 5. The first few readings would often fall above the fit, indicating that a small delay may preceed the initiation of nucleation (see Appendix I).

For all curves the fit was initially performed considering the order of nucleation (n) as a free parameter. The estimated n ranged from 3.78 to 4.17. All fits were then repeated by setting n to the nearest integer (always 4), and the new fits always gave mean square errors less than 1% in excess with respect to fits with free n.[5] The value $n = 4$ corresponds to the nucleation order reported by Tobacman and Korn (1983) as the value which would fit curves with several concentrations of G-actin while keeping K_n constant.

An example of normal polymerization, with superimposed fit, is shown in the *upper panel* of Fig. 1. In the *lower panel* the actin monomer binding rate of the system (excess monomer disappearance rate) is reported with the corresponding

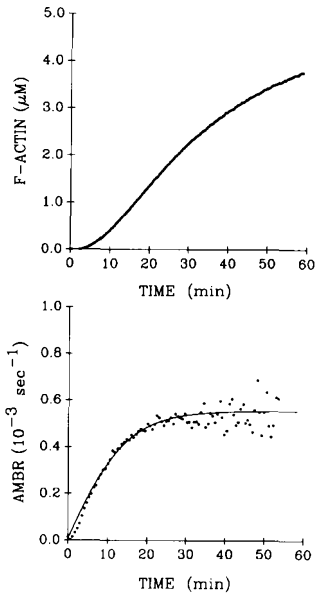

FIG. 1. **Time course of actin polymerization.** Nucleating salts (30 mM KCl, 1 mM $MgCl_2$) were added at time = 0–5 μM G-actin in LIS conditions. In the *upper panel*, changes in fluorescence intensity were transformed into F-actin concentrations by using the experimentally determined critical concentration (0.25 μM; Benfenati *et al.*, 1992). The *lower panel* shows the time course of fractional reduction of G-actin concentration per unit of time, which is referred to as the disappearance rate or AMBR of the system. Note that the disappearance rate starts from zero (no nuclei present at time 0) and rises almost linearly at the beginning (the slope reflecting the initial rate of nucleation); afterwards, the increase in disappearance rate slows down with time until it reaches the final plateau (no more nucleation).

fit. The values obtained for asymptotic disappearance rates (final number of filaments times the association rate constant) were in the range $(5.6–8.3)\cdot 10^{-4}$ s^{-1} (seven curves). The compound nucleation rate constant $(K^+\cdot K_n)$ was in the range $(0.984–2.250)\cdot 10^{15}$ s^{-2} M^{-4}. All curves, either in control or experimental conditions, were generally faster on the first day with a fresh preparation of G-actin and slowed down on the following days; accordingly, all rate constants were higher with fresh preparations and decreased on the following days. As expected, during normal polymerization the disappearance rate monotonically increases from zero to an asymptotic plateau, monitoring the concentration of nuclei and filaments. Its rate of increase is maximal at time 0 and monotonically decreases, indicating that nucleation is initially faster and slows down as the G-actin concentration decreases.

Fig. 2 shows fluorometric measurements (*upper panel*) and disappearance rate (*lower panel*) together with the respective fits, for the polymerization of 5 μM G-actin in the presence of F-actin "seeds." Notice that the disappearance rate starts from a value > 0 and further increases to reach a plateau.

Effects of Synapsin I on Polymerization in the Absence of K^+/Mg^{2+}—When synapsin I is added to G-actin, fluorescence increases, suggesting polymerization, even in the absence of KCl and $MgCl_2$, and the plateau value of fluorescence reached is roughly proportional to the concentration of synapsin I and relatively independent of the concentration of G-actin in the range 1–5 μM (see Valtorta *et al.*, 1992). Under these conditions, the time course of polymerization is roughly bi-exponential (Fig. 3, *upper panels*) and especially so for the highest concentrations of G-actin; disappearance rates start from values correlated with the synapsin I concentration and monotonically decrease (Fig. 3, *lower panels*), suggesting stoichiometric binding of G-actin to synapsin I (with excess concen-

[4] Note that for complex systems mathematical analysis of the kinetic behavior cannot help in selecting among similar models, as small differences in the models would lead to equally good fits with slightly different values for the parameters of the fits.

[5] As a single exception, one curve where n had been estimated at 4.41 could be fitted by $n = 4$ with a 14% increase in the mean square error.

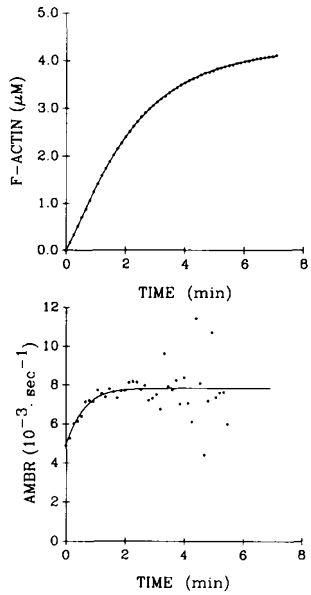

FIG. 2. **Time course of actin polymerization in the presence of F-actin seeds.** *Upper panel*, fluorescence data, obtained after the addition of F-actin seeds to 5 μM G-actin in LIS, were transformed into F-actin concentrations. The respective disappearance rate values and fit are shown in the *lower panel* (AMBR). The initial rise in disappearance rate indicates that further nucleation occurs at early times. F-actin seeds were prepared as described in Valtorta *et al.* (1992).

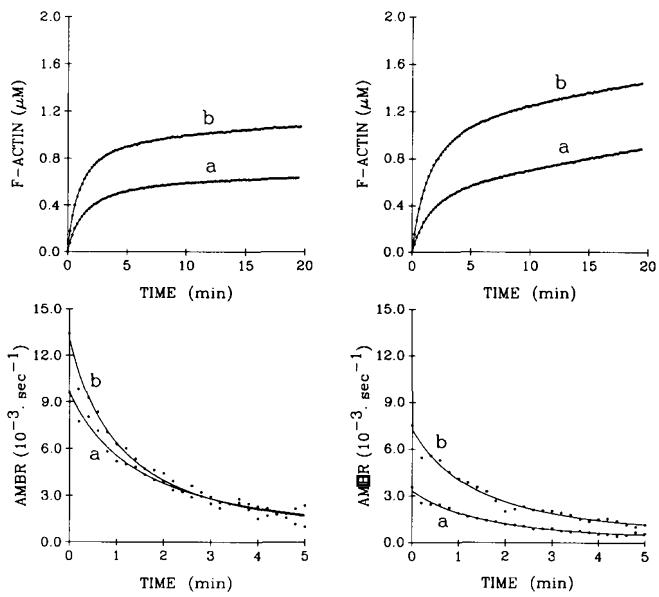

FIG. 3. **Time courses of actin polymerization induced by synapsin I in the absence of K^+/Mg^{2+}.** The time course of actin polymerization (*upper panels*) and disappearance rate (AMBR, *lower panels*) were analyzed following the addition of either 150 nM (*a*) or 300 nM (*b*) synapsin I to a LIS solution containing either 2.5 μM (*left panels*) or 7.5 μM (*right panels*) G-actin, in the absence of K^+/Mg^{2+}. Note that the initial AMBR increases with the synapsin I concentration and that the disappearance rate monotonically decreases with time, suggesting that the process follows the general kinetics of the binding of a ligand in excess to a saturable receptor. Significant further elongation of filaments seems to occur at 7.5 μM G-actin, as suggested by the persistent slope in fluorescence (*upper right panel*).

tration of actin), followed by slow elongation of the complexes. It seemed therefore possible that spontaneous nucleation did not occur to any significant extent but, after monomer binding to synapsin I, the complexes behaved as "nuclei" or filaments and could further elongate, although toward a critical concentration higher than that observed with K^+/Mg^{2+} (0.25 μM, see Valtorta *et al.*, 1992; Benfenati *et al.*, 1992). This hypothesis is strengthened by the observation that, in the presence of actin seeds, G-actin polymerizes even with exceedingly low concentrations of K^+/Mg^{2+}.

Such a kinetic model is described by the following (Scheme V,

$$\begin{cases} S + A \underset{k_0}{\overset{k}{\rightleftharpoons}} SA, & \text{which proceeds to saturation of binding sites S } (k_0 \ll k) \\ P_l + A \underset{k^-}{\overset{k^+}{\rightleftharpoons}} PA_{l+1}, & \text{with equilibrium concentration CC} = k^-/k^+ \end{cases}$$

SCHEME V

where P indicates a saturated complex, "pseudonucleus," capable of elongating, and P_l is a "pseudofilament" of order *l*. Provided binding is noncooperative, more than one binding site can exist on each synapsin I molecule and have to be occupied by actin monomers to give rise to a pseudonucleus (P). Neglecting dissociation in the synapsin I + actin reaction,[6] the time derivative of G-actin concentration is $(d/dt)\ A = -k \cdot A \cdot S - k^+ \cdot P \cdot (A - CC)$. Initially the decline in *A* should follow the decline of free synapsin I sites, which is described, according to tight binding kinetics, by Equation A10 (Appendix II). Once synapsin I sites are saturated, the free monomer concentration should decay to its asymptotic value C (the minimum value between CC and the initial excess of G-actin with respect to binding to synapsin I, $A_0 - S_0$) with rate constant $k^+ \cdot P_\infty$. The precise time course of P is unknown, as pseudonuclei may either self-associate or elongate.

For $c = (A_0 - S_0) \cdot k$, $p = k^+ \cdot P_\infty$, and $a = 1 - S_0/A_0$, the biochemical model (Scheme V) is closely approximated by the following equation,

$$A = [C + (A_0 \cdot a - C) \cdot e^{-pt}]/[1 - (1 - a) \cdot e^{-ct}]$$

with time derivative $(d/dt)\ A = -k \cdot A \cdot S - p \cdot (A - C - f(t))$. The function f(t) has an initial value close to $A_0 - C$ and decays to zero with rate constant *c* (the rate constant of the complexing phase), so that the second term in the time derivative rises to an asymptotic value $k^+ \cdot P_\infty \cdot (A_0 - C)$ and closely approximates $k^+ \cdot P \cdot (A - C)$ at all times. The relevant physical parameters of the biochemical model are the synapsin I + actin association rate constant, *k*, which should dominate the initial complexing phase, the elongation on and off rate constants, k^+ and k^-, and the asymptotic number of complexes or pseudofilaments capable of elongating, P_∞. Fitting this equation to fluorescence curves yields the parameters: $p = k^+ \cdot P_\infty$ = asymptotic disappearance rate ($k^+ \cdot F_\infty$ in the other models); $A_0 \cdot (1 - a) = S_0$ = "synapsin I driven pool" of actin = binding capacity of synapsin I (from which the stoichiometry of the complex is estimated); $A_0 \cdot a - C$ = "elongation

[6] For tight binding, $(d/dt)A = -k \cdot A \cdot S = -k \cdot A \cdot (A + S_0 - A_0)$, which yields: $A = A_0 \cdot a/[1 - (1 - a) \cdot e^{-ct}]$, where $c = A_0 \cdot a \cdot k$ and $a = (A_0 - S_0)/A_0$. If dissociation is not negligible, then $(d/dt)A = -k \cdot A \cdot S + k_0 \cdot (A_0 - A)$, and A reaches equilibrium at $A_\infty = \{A_0 - S_0 - K_D + \sqrt{[(A_0 - S_0 - K_D)^2 + 4 \cdot A_0 \cdot K_D]}\}/2$, where $K_D = k_0/k$. By setting $\mathscr{A} = A + \{\sqrt{[(A_0 - S_0 - K_D)^2 + 4 \cdot A_0 \cdot K_D]} - (A_0 - S_0 - K_D)\}/2$, $a' = \mathscr{A}_\infty/\mathscr{A}_0$ and $\mathscr{A}_\infty = \sqrt{[(A_0 - S_0 - K_D)^2 + 4 \cdot A_0 \cdot K_D]}$, the same equation results, with $\mathscr{A}$ in place of A and a' in place of *a*. Note that the fluorescence, which monitors $A_0 - A = \mathscr{A}_0 - \mathscr{A}$, will therefore be fit by the same equation as for tight binding, although the constants in the equation will be modified: apparent G-actin initial concentration $\mathscr{A}_0 \geq A_0$, apparent synapsin I initial concentration $S'_0 \leq S_0$, apparent synapsin I-independent pool $a' = \mathscr{A}_\infty/\mathscr{A}_0 \geq A_\infty/A_0$. The equalities are approached as $K_D \to 0$.

pool," *i.e.* the pool of actin polymerized independently of complexing with synapsin I; $k = c/(A_0 \cdot a)$ = synapsin I + G-actin association rate constant.

When this model was used to fit actin polymerization curves obtained with synapsin I in the absence of K^+/Mg^{2+} the fits were excellent (Fig. 3, *upper panels*). However, this does not exclude that concurrent spontaneous nucleation might occur, although at a very slow rate, so that the apparent equilibrium approached by these curves may not be the true long-term equilibrium under these conditions.

Table I summarizes the results obtained with various concentrations of G-actin and synapsin I. The experiments with 2.5 and 5 μM G-actin gave initial disappearance rates and asymptotic concentrations of F-actin dependent on synapsin I concentration only. From the pooled data the association rate constant for the reaction G-actin/synapsin I can be estimated to $1.5\text{–}12 \cdot 10^3$ $M^{-1} \cdot s^{-1}$. The binding of G-actin to synapsin I appears to follow a stoichiometry 1:2–4 (1:3–4 was the value experimentally determined in the accompanying paper, Valtorta *et al.*, 1992).

With 1 μM G-actin and 300 nm synapsin I, the estimated elongation pool was close to zero and the curve was perfectly fitted by exact stoichiometry ligand-receptor binding kinetics alone, $A = A_0/(1 + A_0 \cdot k)$, with association rate constant $k = 12 \cdot 10^3$ M^{-1} s^{-1}. A small elongation pool of actin (0.2–0.5 μM) was estimated for initial concentrations ≤5 μM, relatively insensitive to actin concentration and higher for 300 nM synapsin I. The elongation pool was larger with 7.5 μM G-actin; polymerization proceeded to about 1.5 μM F-actin, independently of synapsin I concentration, suggesting a CC close to 6 μM, in agreement with the observation that actin complexing/polymerization under these conditions had a clearly biphasic time course, as if it proceeded well beyond saturation of synapsin I, when the initial G-actin concentrations exceeded 5 μM (Valtorta *et al.*, 1992). The presence of a roughly constant extent of elongation with G-actin concentrations lower than this estimated CC might be explained by an initially higher value for k^+, as would be the case if the filaments were stabilized, as long as free synapsin I was available, by lateral binding of synapsin I (Bähler and Greengard, 1987; Petrucci and Morrow, 1987; Benfenati *et al.*, 1992). In this case, some synapsin I could be subtracted by growing filaments and synapsin I binding capacity (and stoichiometry of complexing) could be underestimated.

These results suggest that elongation occurs on nuclei or pseudonuclei under conditions where no "spontaneous" polymerization (nucleation + elongation) appears to occur. However, the estimated asymptotic fluorescence and free monomer concentration agree with pelleting data obtained at 20 min, but not after 2 h (Valtorta *et al.*, 1992). This suggests that either a slower elongation process ensues at late times or nucleation is delayed and slow but does occur under these conditions. Thus, kinetic fits on the fast polymerization phase of these experiments yield information on the synapsin I driven processes that are fast enough to approach an apparent equilibrium within 20 min, but may miss much slower processes that determine the final equilibrium state and do not significantly affect these early kinetics.

Effect of Synapsin I on the Polymerization of G-actin in the Presence of K^+/Mg^{2+}—In the presence of K^+/Mg^{2+}, synapsin I induces a biphasic behavior of excess monomer disappearance rates (AMBR in Figs. 4 and 6). The disappearance rate starts above zero, decreases, and then rises again to plateau. With increasing concentrations of synapsin I the initial disappearance rate increases, whereas its final value decreases (Fig. 4, *lower panel*). Thus, binding sites for G-actin appear to be present from the beginning and to become saturated soon, whereas spontaneous nucleation concurrently occurs. These data imply that: (i) synapsin I can rapidly bind actin monomers and change their conformation so as to make the pyrene residue fluoresce (as indicated by the initial AMBR > 0), (ii) it can behave as a nucleus/filament, and (iii) it produces filaments with slower elongation than normal.

This model for synapsin I and G-actin interaction is the simplest one that can account for all the experimental observations. The corresponding biochemical system is analyzed in Appendix II, yielding the final Equation 9 reported under the "Theory" section. Using the model of Equation 9, polymerization curves of 5 μM G-actin in the presence of various concentrations of synapsin I were fitted, and the pool of actin complexed/polymerized by synapsin I was estimated to 4%, 7–8%, and 25–34% for 50, 100, and 300 nM synapsin I, respectively. Thus, the stoichiometry for the synapsin I-dependent complexing/polymerization appears to be 1:3–5 synapsin I:actin. The effects of various concentrations of synapsin I on the kinetic parameters of actin polymerization (tested on the same day) are reported in Fig. 5. The final rate constant for polymerization ($K^+ \cdot F_\infty$ = asymptotic disappearance rate) decreased with increasing concentrations of synapsin I, suggesting that the filaments formed by synapsin I, and possibly all filaments in the presence of synapsin I, elongate more slowly. Similarly, the compound nucleation rate constant ($K^+ \cdot K_n$) decreased with increasing concentrations of synapsin I. This suggests a marked decrease in K^+, rather than in the nucleation rate constant, K_n, as the final number of filaments, F_∞, should slightly increase under this condition (Benfenati

TABLE I

Effects of synapsin I on actin polymerization in the absence of K^+ and Mg^{2+}

All curves were performed on the same day in buffer A containing 15 mM NaCl. $K^+ \cdot P_\infty$ is the final AMBR; k is the actin/synapsin I association rate constant. The asymptotic free monomer concentration equals the minimum value between CC and the excess G-actin with respect to stoichiometry to synapsin I. *, this curve was fitted assuming exact stoichiometric binding. All concentration values were obtained by scaling the asymptotic fluorescence value with 1 μM G-actin + 300 nM synapsin I to 1 μM.

G-actin	Synapsin I	$K^+ \cdot P_\infty$	Synapsin I-driven pool	Elongation pool	Asymptotic-free monomer concentration	k
μM	nM	$10^{-3} \cdot s^{-1}$	μM	μM	μM	$10^3 \cdot M^{-1}\ s^{-1}$
1.0	300	=	1.0	0 (*)	0 (*)	12
1.0	150	2.2	0.40	0.21	0.39	14
2.5	300	1.9	0.73	0.34	1.43	7.3
2.5	150	2.4	0.39	0.25	1.86	6.0
5.0	300	1.5	0.62	0.48	3.90	4.6
5.0	150	1.7	0.38	0.23	4.37	3.3
7.5	300	1.2	0.83	0.78	5.89	1.8
7.5	150	0.5	0.44	1.03	6.03	1.5

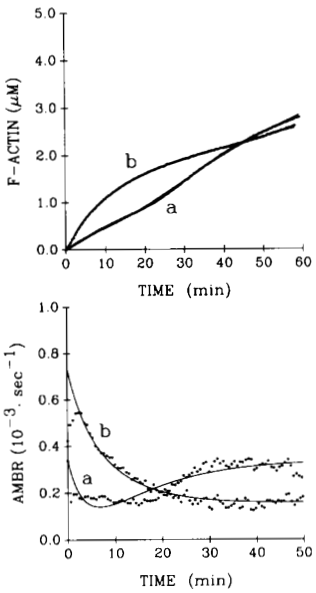

FIG. 4. **Time course of actin polymerization induced by K^+/Mg^{2+} in the presence of synapsin I.** The *upper panel* shows the changes in F-actin concentration in the presence of either 100 nM (*a*) or 300 nM (*b*) synapsin I, added to 5 μM G-actin in LIS together with nucleating salts (30 mM KCl, 1 mM $MgCl_2$). The corresponding time courses of disappearance rate (AMBR) are shown in the *lower panel*. Note the high initial values of AMBR (correlated with the concentration of synapsin I) and its rapid decrease. The late increase (particularly evident with 100 nM synapsin I) indicates that nucleation occurs, although it is slowed down with respect to control conditions by the marked sequestration of G-actin during the initial phase of synapsin I-driven polymerization.

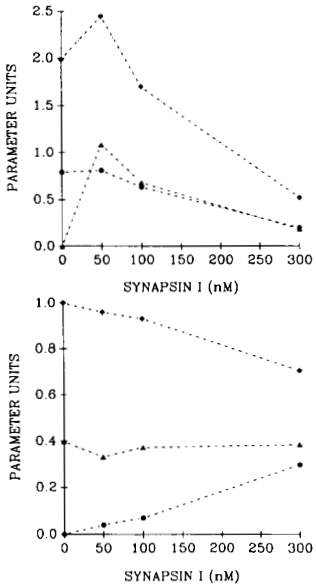

FIG. 5. **Changes in the parameters of actin polymerization as a function of the concentration of synapsin I.** *Upper panel*: ●, asymptotic disappearance rate = $K^+ \cdot F_\infty$ ($10^{-3} \cdot s^{-1}$), F_∞ being the final number of filaments; ♦, compound nucleation rate constant = $K^+ \cdot K_n$ ($10^{15} \cdot s^{-2}\ M^{-4}$); ▲, G-actin/synapsin I association rate constant = k ($10^3 \cdot M^{-1}\ s^{-1}$). *Lower panel*: ●, synapsin I-driven pool (fraction of the total initial G-actin concentration) = $(1 - a^{2/n})$; ♦, residual pool (fraction of the total); ▲, ratio F_∞/K_n ($10^{-18} \cdot M^{-4}$), indicating the change in the final number of filaments induced by synapsin I, assuming that the nucleation rate constant is not affected. The lack of a marked change in this ratio indicates that a decrease in the association rate constant for actin monomers to actin filaments (K^+) accounts for the decrease in the elongation rate induced by synapsin I.

et al., 1992). Consistently, the ratio F_∞/K_n remains constant with the various concentrations of synapsin I. Stoichiometric binding of synapsin I to G-actin is strongly suggested by the changes in synapsin I-driven and residual pools with respect to synapsin I concentration. The rate constant for the stoichiometric G-actin/synapsin I association (k) was in the range $(0.2–1.1) \cdot 10^3\ M^{-1}\ s^{-1}$ and was inversely related to the synapsin I concentration. This suggests that the binding kinetics are more complex than simple stoichiometric ligand-receptor kinetics and that the G-actin/synapsin I concentration ratio may influence the interaction.

The observed stoichiometry (1:3–5) is consistent with the stoichiometry deduced from polymerization curves in the presence of synapsin I without K^+/Mg^{2+} (1:2–4, see above, or 1:3–4, Valtorta *et al.*, 1992), but differs from the previously reported values for the stoichiometry of synapsin I binding to preformed actin filaments (1:7–10 synapsin I:F-actin; Bähler and Greengard, 1987; Bähler *et al.*, 1989). However, this would merely imply that synapsin I interacts differently with G-actin than with F-actin.

Clearly, the real situation might well be more complicated than described by this model (Equation 9); further information from additional physical techniques may help in clarifying the nature of the intermediate structures involved in the complex interaction between synapsin I and actin.

Modulation of the Effects of Synapsin I by Ionic Strength and Phosphorylation—Polymerization and disappearance rate curves obtained with 0 or 300 nM synapsin I in the absence of Ca^{2+} (Ca^{2+} buffered at 10^{-9} M with EGTA) are illustrated in Fig. 6 (*upper* and *lower panels*, respectively). The estimated sizes of synapsin I-driven and -independent pools were similar to the corresponding values observed in the presence of 10^{-4} M Ca^{2+} (see Table II), and the synapsin I/G-actin association

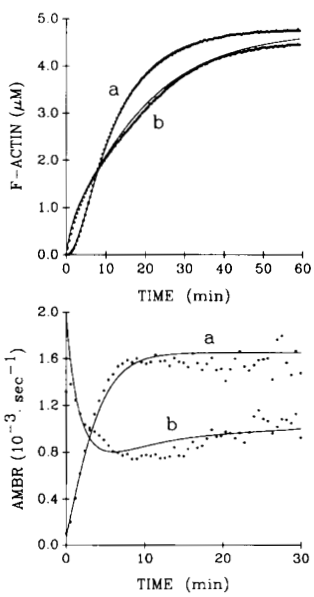

FIG. 6. **Time course of actin polymerization in "Ca^{2+}-free" solution.** The *upper panel* shows the change in F-actin concentration either in the absence (*a*) or in the presence (*b*) of 300 nM synapsin I in LIS. Ca^{2+} was buffered to 10^{-9} M with EGTA added 10 min before polymerization was started. The *lower panel* illustrates the corresponding time courses of disappearance rate (AMBR). Note that the effect of synapsin I is qualitatively the same as in Fig. 3, although the whole process is noticeably faster in the absence of Ca^{2+}.

TABLE II

Modulation of the effects of synapsin I by Ca^{2+} and ionic strength

All curves were performed on the same day in buffer A containing: LIS, 15 mM NaCl, 30 mM KCl, 1 mM $MgCl_2$; Ca^{2+}-free, the same as LIS but with Ca^{2+} buffered to 10^{-9} M with EGTA: HIS, 85 mM NaCl, 30 mM KCl, 1 mM $MgCl_2$. $K^+ \cdot F_\infty$ is the final AMBR; $K^+ \cdot K_n$ is the compound nucleation rate constant; k is the G-actin/synapsin I association rate constant. Residual pool indicates the fraction of G-actin undergoing spontaneous polymerization.

	$K^+ \cdot F_\infty$	$K^+ \cdot K_n$	k	Residual pool
	$10^{-3} \cdot s^{-1}$	$10^{15} \cdot s^{-2} M^{-4}$	$M^{-1} s^{-1}$	%
A. LIS conditions				
G-actin (5 μM)	0.555	0.984		100
+synapsin I (300 nM)	0.229	0.530	137	75
B. Ca^{2+}-free conditions				
G-actin (5 μM)	1.710	9.304		100
+synapsin I (300 nM)	0.923	7.773	423	77
C. HIS conditions				
G-actin (5 μM)	0.468	0.700		100
+synapsin I (300 nM)	1.270	19.125	340	72

rate constant reached values generally obtained with lower concentrations of synapsin I in the presence of Ca^{2+}. This suggests faster synapsin I/G-actin interaction in Ca^{2+}-free solution. Indeed, the time scale of the whole process appears to be accelerated: without synapsin I, $K^+ \cdot K_n$ increases by a factor of 10 and $K^+ \cdot F_\infty$ by a factor of 3; with 300 nM synapsin I the two rate constants increase by factors of 15 and of 4.6, respectively (Table II).

The sensitivity of the effect of synapsin I to changes in ionic strength was examined. In high ionic strength buffer (85 mM NaCl, 30 mM KCl, 1 mM $MgCl_2$), actin polymerization was extremely fast with 300 nM synapsin I; however, the sizes of the two pools of actin were the same as under low ionic strength conditions. The G-actin/synapsin I association rate constant was increased to values similar to those observed in Ca^{2+}-free solutions.

As mentioned in the accompanying paper (Valtorta *et al.*, 1992), under low ionic strength conditions phosphorylation reduced the ability of synapsin I to accelerate actin polymerization and to suppress the initial lag; however, with 300 nM synapsin I the G-actin disappearance rate started from values >0 and the model of Equation 9 with 70–75% "synapsin I-independent pool" could fit the polymerization curves (not shown). Under high ionic strength conditions, the effects of phosphorylation were more dramatic; the initial lag was not abolished and the disappearance rate had the usual time course observed for G-actin alone (*i.e.* AMBR started from zero and monotonically rose to reach a plateau) (not shown). However, in the presence of phosphorylated synapsin I, the whole process was slightly faster than without synapsin I, especially when synapsin I was phosphorylated on site 1.

Effects of Synapsin I on the Polymerization Driven by F-actin Seeds with Low K^+/Mg^{2+}—Polymerization of G-actin proceeds slowly in the presence of very low concentrations of K^+/Mg^{2+} (Attri *et al.*, 1991). When F-actin seeds are added under these conditions (15 mM NaCl, 3 mM KCl, 0.1 mM $MgCl_2$), actin polymerizes at high speed (Flanagan and Lin, 1980; see also Valtorta *et al.*, 1992). It was of interest to investigate whether polymerization under these conditions was fully accounted for by elongation of preexisting filaments or whether some nucleation occurred. The disappearance rates shown in Fig. 7 (*upper panel*) indicate that, in the absence of synapsin I, no significant nucleation occurs with seeds and low K^+/Mg^{2+} during the first 30 min (the AMBR remains constant throughout the polymerization, *curve a*). Subtraction of monomers by active elongation of seeds presumably contributes to lowering the rate of nucleation. Dephosphosynapsin I, as usual, behaves as a saturable binding site for G-actin (AMBR monotonically decreases from an initial value higher than that obtained with seeds only) and decreases the overall elongation rate (*curve b*). Synapsin I phosphorylated on sites 2 and 3 (*curve c*) has a similar behavior, although its effect is weaker; the initial disappearance rate is smaller, but the decrease in the elongation rate is similar to that observed with dephosphosynapsin I.

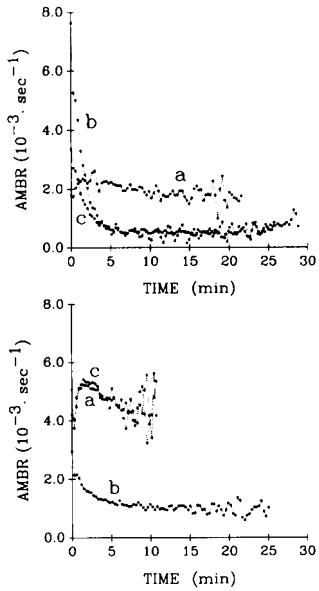

FIG. 7. **Effect of synapsin I on the AMBR in the presence of F-actin seeds at low concentration of K^+/Mg^{2+}.** F-actin seeds were added to 5 μM G-actin at low concentration of nucleating salts (3 mM KCl, 0.1 mM $MgCl_2$), in the absence of synapsin I (*a*), in the presence of dephosphorylated synapsin I (*b*), or in the presence of synapsin I phosphorylated on sites 2 and 3 by CaM kinase II (*c*). The experiments were carried out under LIS (*upper panel*) or HIS (*lower panel*) conditions. The corresponding time courses of actin polymerization are depicted in Fig. 9 of the accompanying paper (Valtorta *et al.*, 1992). Notice that no nucleation (*i.e.* no increase in disappearance rate) appears to occur under any condition and that phosphorylation reduces the effect of synapsin I under LIS and abolishes it under HIS.

When the ionic strength is elevated by adding 70 mM NaCl (Fig. 7, *lower panel*), the time courses of disappearance rate are similar to those observed under low ionic strength for seeds alone (*curve a*) and seeds + dephosphosynapsin I (*curve b*), whereas synapsin I phosphorylated on sites 2 and 3 (*curve c*) appears to be ineffective. These data are consistent with those reported above and in the accompanying paper (Valtorta *et al.*, 1992), indicating that under high ionic strength conditions synapsin I phosphorylated on sites 2 and 3 loses its activity on actin polymerization.

Use of Disappearance Rates in Interpreting Polymerization Curves—The transformation of fluorescence data into AMBR values provides clues as to the effects produced on actin polymerization by changes in the experimental conditions. As discussed above, differences among the kinetics under the conditions examined in this study, and departures from "normal" polymerization, are clearly focussed in the plots of excess monomer disappearance rates.

The disappearance rate analysis was carried out also on data of actin polymerization in the presence of brevin (taken from Doi and Frieden, 1984) or *Acanthamoeba* capping protein (taken from Cooper and Pollard, 1985). With brevin (Fig. 8, *left panels*), effects similar to those induced by synapsin I in the absence of K^+/Mg^{2+} were observed; thus, brevin displays

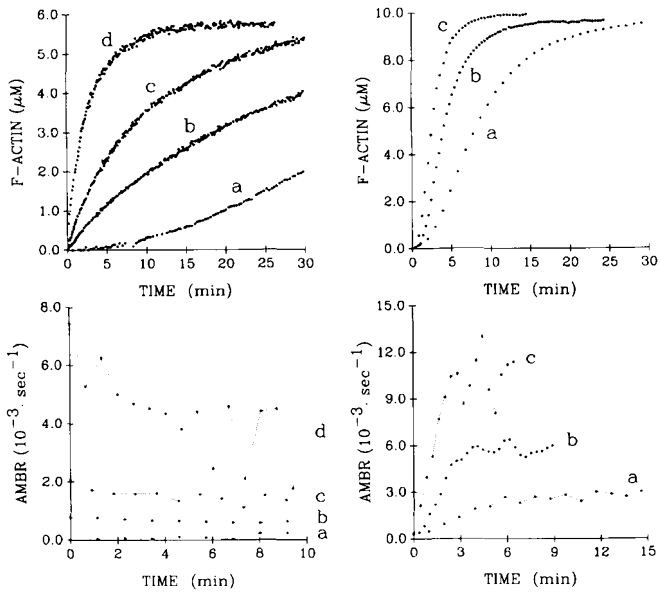

FIG. 8. **Changes in AMBR induced by brevin and *Acanthamoeba* capping protein.** The *upper left panel* reproduces curves obtained by polymerizing 5.87 μM G-actin in the absence (*a*) or in the presence of 19.6 (*b*), 58.7 (*c*), or 196 (*d*) nM brevin (Doi and Frieden, 1984). The *lower left panel* shows the corresponding time courses of disappearance rate (AMBR). Similarly to the curves obtained with synapsin I in the absence of K^+/Mg^{2+} (Fig. 5; see also Figs. 4 and 7 in the accompanying paper (Valtorta *et al.*, 1992)), the initial AMBR is high and monotonically decreases during polymerization. However, the final AMBR is higher than that reached without brevin and correlated with the concentration of brevin. This suggests that brevin-driven polymerization is partly saturable (as appears to be the case with synapsin I), but that the complexes actively elongate so that the process proceeds to equilibrium faster than in the absence of brevin (at variance with the decrease in the rate of elongation observed with synapsin I). The *upper right panel* reproduces curves obtained by polymerizing 10 μM G-actin in the presence of 0 (*a*), 330 (*b*), or 1040 (*c*) nM *Acanthamoeba* capping protein (Cooper and Pollard, 1985). The *lower right panel* shows the corresponding time courses of disappearance rate, indicating that the capping protein induces a dose-dependent acceleration of nucleation (initial slope of the AMBR), but it does not behave as a nucleus (zero initial AMBR).

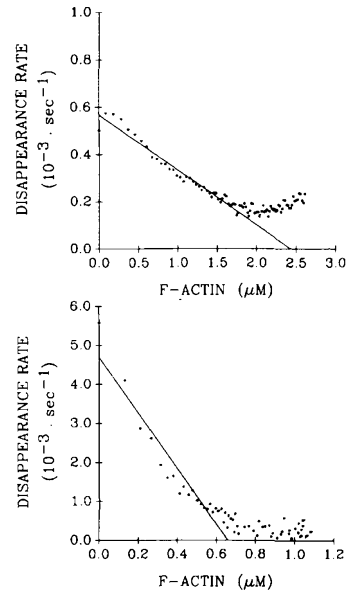

FIG. 9. **Relationship between disappearance rate and increase in actin fluorescence.** The actin monomer disappearance rate is plotted *versus* fluorescent actin. Both panels show data obtained with 5 μM G-actin and 300 nM synapsin I; either 1 mM Mg^{2+}, 30 mM K^+ (*upper panel*) or no K^+/Mg^{2+} (*lower panel*) were present. If the increase in fluorescence is initially dominated by stoichiometric binding to synapsin I, then the disappearance rate is initially proportional to the binding capacity of synapsin I and decreases linearly with the increase in fluorescent actin, with negative slope equal to the association rate constant. Notice that for these plots tight binding is assumed (no critical concentration) and disappearance rates of G-actin (rather than excess monomer with respect to CC) are considered. The linear regression intercepts the *abscissa* at a value corresponding to the total binding capacity of synapsin I. The association rate constants estimated from the negative slopes are: 233 $M^{-1} \cdot s^{-1}$ (*upper panel*) *versus* the analytically fitted value of 181 $M^{-1} \cdot s^{-1}$; 7,100 $M^{-1} \cdot s^{-1}$ (*lower panel*) *versus* a fitted value of 4,500 $M^{-1} \cdot s^{-1}$ (see Table I).

nucleating activity and impairs spontaneous nucleation (although the latter might simply be too fast to give rise to a separate late increase in disappearance rate). In the presence of *Acanthamoeba* capping protein (Fig. 8, *right panels*), the disappearance rate starts from zero as in normal polymerization, but then rises to plateau with a speed proportional to the protein concentration, suggesting that the protein accelerates nucleation, behaving as a "prenucleus" or an activator of low order actin complexes (as proposed by Cooper and Pollard, 1985).

The model proposed in this study for G-actin/synapsin I interaction predicts that the initial part of fluorometric curves should be dominated by stoichiometric binding of G-actin to synapsin I. If this is true, then the initial disappearance rate will be mostly accounted for by the product $k \cdot S$ and will decrease linearly with the increase in fluorescence. This is shown by plotting the monomer disappearance rate *versus* the increase in fluorescence, as in Fig. 9 (note that in this case G-actin concentration rather than its excess with respect to the asymptotic value has been considered, as for tight binding there is no equilibrium concentration). The slopes of the linear regressions yield estimates of k in reasonable agreement with the results of the analytical fit. Without K^+/Mg^{2+}, the intercept on the *abscissa* indicates a total binding capacity close to 0.7 μM (corresponding to a 1:2–3 stoichiometry); in the presence of K^+/Mg^{2+} this value is increased to 2.4 μM, due to the contribution of concurrent nucleation to the disappearance rate.

CONCLUSION

The dissection of the molecular mechanisms involved in the nucleation and elongation of actin filaments would require a systematic analysis of the modifications induced by ions, adenosine nucleotides, temperature, etc. on the actin polymerization process. However, the analytical models developed in this study constitute a "toolbox" to describe and study actin polymerization kinetics under various experimental conditions and to interpret the effects of specific treatments. We have proposed to use in these analyses an operational quantity called actin monomer binding (disappearance) rate; this parameter monitors the combined activities of actin filaments, seeds, and actin-binding proteins, thus helping in defining the mechanisms of the interference with the actin polymerization process.

The quantitative results of this study substantiate the suggestion that synapsin I interacts in a complex way with actin: (i) synapsin I appears to be able to bind actin monomers and change their conformation as if they had been incorporated in a nucleus/filament; the pseudo-nucleus formed appears to be able to elongate; thus, synapsin I behaves as a nucleating protein in the sense that it "generates" nuclei, rather than favoring nucleation by activating intermediate aggregates, as reported for other nucleating proteins (Doi and Frieden, 1984; Cooper and Pollard, 1985). At variance with classical nucleat-

ing proteins (*e.g.* Glenney *et al.*, 1981), synapsin I displays a high stoichiometry (1:2–4) in its binding to G-actin. It may be observed that nucleating proteins contain domains with high sequence homology (Vandekerckhove, 1989); consistent with the functionally different interaction of synapsin I with actin, synapsin I has no significant homology with other nucleating proteins (Südhof *et al.*, 1989). (ii) As is the case for other nucleating proteins, synapsin I decreases the final elongation rate of actin filaments; however, at variance with the "capping" property of many nucleating proteins which, by binding to the barbed end of the filament, slow down elongation and increase the critical concentration (*e.g.* Isenberg *et al.*, 1980; Yin *et al.*, 1981), synapsin I decreases the critical concentration (Benfenati *et al.*, 1992). The decrease in the elongation rate constant is therefore likely to be related to phenomena different from capping (*e.g.* bundling of actin filaments). (iii) The effects of synapsin I occur independently of the presence of Ca^{2+}. (iv) The effects of synapsin I are qualitatively similar independent of ionic strength, indicating that they do not arise from nonspecific interactions. (v) The effects of synapsin I are markedly dependent on its state of phosphorylation.

All these observations, combined with the notion that synapsin I can specifically interact with synaptic vesicles (Huttner *et al.*, 1983; Schiebler *et al.*, 1986; Benfenati *et al.*, 1989), support the view that synapsin I may play a major role, modulated by phosphorylation, in the dynamics of the cytoskeletal matrix of the nerve terminal, thereby regulating the availability and mobility of synaptic vesicles during active release of neurotransmitter (Bähler *et al.*, 1990; De Camilli *et al.*, 1990; Benfenati *et al.*, 1991).

Acknowledgments—We thank the reviewers for their helpful comments and for the careful and detailed analysis of the manuscript.

APPENDIX I: ACTIN NUCLEATION

Let the association rate constant between two actin monomers be α_1 and the dissociation rate constant β_1; similarly, let the association rate constant for monomer + jth order oligomer be α_j and the corresponding dissociation rate constant β_j. Indicating the concentration of jth order oligomers by A_j, we have the following.

$$(d/dt)A_2 = \alpha_1 \cdot A_1^2 - \beta_1 \cdot A_2 + \beta_2 \cdot A_3 \quad (A1)$$

Initially, when higher order oligomers are not present, the last term can be neglected, yielding the following,

$$(d/dt)A_2 = \alpha_1 \cdot A_1^2 - \beta_1 \cdot A_2, \quad (A2)$$

and in general,

$$(d/dt)A_j = \alpha_{j-1} \cdot A_{j-1} \cdot A_1 - \beta_{j-1} \cdot A_j. \quad (A3)$$

The solution to this equation can be stated as follows: A_{j+1} equals $(\alpha_j/\beta_j) \cdot A_j \cdot A_1$, after filtering by an impulse response $\beta_j \cdot \exp(-\beta_j t)$, *i.e.* for any value of j, A_{j+1} reaches equilibrium at $A_{j+1} = A_j \cdot A_1 \cdot (\alpha_j/\beta_j)$ and follows the time course of A_j as a lowpass filter with rate constant β_j. Since initially no oligomers (or nuclei) are present, and nuclei are subtracted from the system by further elongation, the system can be modeled by considering only equilibration of oligomers with lower order oligomers and monomers. This yields the following system,

$$A_j = (\alpha_{j-1}/\beta_{j-1}) \cdot A_{j-1} \cdot A_1 * \beta_{j-1} \cdot \exp(-\beta_{j-1} t) \quad (A4)$$

$$A_j = [(\alpha_1 \cdot \alpha_2 \cdot \ldots \cdot \alpha_{j-1})/(\beta_1 \cdot \beta_2 \cdot \ldots \cdot \beta_{j-1})] \cdot A_1^j * H_j(t) \quad (A5)$$

where "*" indicates convolution (filtering), and $H_j(t)$ is the result of convolving the functions $\beta_1 \exp(-\beta_1 t) * \beta_2 \exp(-\beta_2 t) * \ldots * \beta_{j-1} \exp(-\beta_{j-1} t)$. If all β_j values are equal, then $H_j(t)$ is a $(j-1)$th order γ distribution function with unit area and time to the peak $\tau = (j-1)/\beta$. For different αs and βs, the equilibrium concentration for A_j still equals $[(\alpha_1 \cdot \alpha_2 \cdot \ldots \cdot \alpha_{j-1})/(\beta_1 \cdot \beta_2 \cdot \ldots \cdot \beta_{j-1})] \cdot A_1^j$ and A_j will follow A_1^j with a time-delay comparable with D = sum $(1/\beta_i, i = 1, j-1)$. Therefore the concentration of highest-order unstable oligomers (oligomers of order $n-1$) will be proportional to $[(\alpha_1 \cdot \alpha_2 \cdot \ldots \cdot \alpha_{n-2})/(\beta_1 \cdot \beta_2 \cdot \ldots \cdot \beta_{n-2})] \cdot A_1^{n-1} = K \cdot A^{n-1}$, not considering the above-mentioned time delay; when the nucleus is favored to grow and nucleus breakage can be neglected, the nucleation (=net increase in number of nuclei per unit of time) is described by the following,

$$(d/dt)A_n = \alpha_{n-1} \cdot A_{n-1} \cdot A_1 = K \cdot \alpha_{n-1} \cdot A_1^n = K_n \cdot A_1^n \quad (A6)$$

where K_n can be called nucleation rate constant ($M^{-(n-1)}\ s^{-1}$), again not considering a time delay. When the G-actin concentration approaches the critical concentration, CC, newly formed nuclei tend to accumulate and are no more favored to grow, so $(d/dt)A_n \rightarrow 0$. To account for this, Equation A6 can be modified by substituting $X = (A_1 - CC)$ for A_1, *i.e.* $(d/dt)A_n = K_n \cdot X^n$.

Equation A6 could generally be used to accurately fit data of actin polymerization. However, in experiments performed in Ca^{2+}-free solutions, the initial part of the curves would often appear to be delayed with respect to analytical curves obtained as described in the methods using Equation A6 to model nucleation, and much better fit would be obtained by introducing in the equation a delaying filter with impulse response described by a $(n-1)$th order γ distribution function. It may be observed that in the initial time interval D, a number of filaments about equal to $D \cdot K_n \cdot (A_0 - CC)^n$ (A_0 = initial G-actin concentration) would be formed, if no delay were present; this amounts to a fraction $D \cdot K_n \cdot (A_0 - CC)^n / F_\infty$ of the total number of filaments formed during polymerization. From Equation 7b, $K_n \cdot (A_0 - CC)^n / F_\infty = p$ (where p is the main rate constant of actin polymerization); thus the error introduced by neglecting the initial delay is proportional to $D \cdot p$. When G-actin is associated with Mg^{2+} rather than Ca^{2+} (see, *e.g.* Frieden, 1985), p rises. Under this condition binding of G-actin is favored, and this implies that dissociation rates (which determine D) do not increase to the same extent as association rates do. Therefore, the product $D \cdot p$ is expected to rise in Ca^{2+}-free solutions, and the error introduced by neglecting the initial delay becomes significant.

APPENDIX II: G-ACTIN/SYNAPSIN I INTERACTION

In the presence of synapsin I, the actin monomer binding rate or G-actin disappearance rate (= negative derivative of the logarithm of excess G-actin) is greater than zero from the beginning; this suggests that synapsin I may account for extra binding capacity. In this case we would have the following,

$$-(d/dt)\log(X) = R(t) = K^+ \cdot \int dt\ K_n \cdot X^n + \phi(t) \quad (A7)$$

where $\phi(t)$ = excess in disappearance rate, $R(t)$, due to binding to synapsin I. Therefore,

$$-(d^2/dt^2)\log(X) = K^+ \cdot K_n \cdot X^n + (d/dt)\phi(t). \quad (A8)$$

An approximate solution to Equation A8 is as follows,

$$X = X_0 \cdot [f/\cosh(g)]^{2/n}, \quad (A9)$$

where $(2/n) \cdot (d/dt)\log(f(t)) = -\phi(t)$, $(d/dt)\ g(t) = p \cdot f(t)/f(\infty)$, and p is a rate constant. Note that for $f(t) \equiv 1$, Equation

A9 reduces to Equation 5 under the "Theory" section. Actually, according to Equation A9, $-(d^2/dt^2)\log(X) = (2p^2X_0^{-n}/n)\cdot X^n + (d/dt)\phi(t) + [2p/n\cdot f(\infty)]\cdot[(d/dt)f(t)]\cdot\tanh(g)$, and the approximation is acceptable provided that the last term can be neglected; this is the case if $(d/dt)f(t)$ approaches zero before $\tanh(g)$ rises significantly from zero, which generally occurs with synapsin I.

The function $f(t)$ must be selected according to the model of G-actin/synapsin I interaction, and considering that $(d/dt)\log(f) = [(d/dt)f]/f$ must follow the time course of the excess in disappearance rate $\phi(t)$. Data on actin polymerization and disappearance rate in the presence of various concentrations of synapsin I, either with or without K^+/Mg^{2+}, and electron microscopy observations (see Valtorta *et al.*, 1992) suggest a stoichiometric binding of G-actin to synapsin I to create filaments. In this case, indicating by S the concentration of binding sites on synapsin I and neglecting dissociation (but see Footnote 6), we would have the following,

$$S = S_0\cdot a\cdot e^{-ct}/[1 - (1 - a)\cdot e^{-ct}] \qquad (A10)$$

where S_0 is the initial concentration of G-actin binding sites on synapsin I, $a = 1 - S_0/A_0$ is the fraction of G-actin in excess with respect to stoichiometry, and $c = A_0\cdot a\cdot k$, where k is the association rate constant (neglecting unbinding).

The function $f(t)$ can therefore be set to $f(t) = a/[1 - (1 - a)\cdot e^{-ct}]$ (solution I), so that $(d/dt)\log(f) = -k\cdot S$, as expected for stoichiometric binding. Actually, from Equation A9 $f^{2/n}(t)$, and not $f(t)$, should equal $a/[1 - (1 - a)\cdot e^{-ct}]$ (solution II). However, the only difference is that, with solution I, $A^{n/2}$ rather than A behaves as the ligand, and this is actually an advantage in modelling stoichiometric binding that occurs concurrently to an independent process ($\int$) that subtracts actin monomers. In fact, in this case

$$(d/dt)\ A = -k\cdot S\cdot A - \int,\ \int = -(d/dt)(A - S); \qquad (A11)$$

$$(d/dt)\ A = -k\cdot S\cdot A + (d/dt)(A - S) \qquad (A12)$$

and

$$(d/dt)\ A^{n/2} = -(n/2)\cdot k\cdot S\cdot A^{n/2} + (n/2)\cdot A^{n/2-1}\cdot(d/dt)(A - S). \qquad (A13)$$

Initially, when A is large, stoichiometric binding dominates, so $\int = (d/dt)(A - S)$ may be negligible; later on, the process $\int$ becomes relevant, but A may have decreased by that time. Under these conditions, the rightmost term can be neglected in Equation A13, which reduces to solution I, but not in Equation A12, which would reduce to solution II.

The analytical equation used to model actin polymerization in the presence of synapsin I was therefore Equation A9 with $f(t) = a/[1 - (1 - a)\cdot e^{-ct}]$ and $(d/dt)g(t) = (p/a)\cdot f(t)$, *i.e.* $g(t) = (p/c)\cdot\log[1 - (1 - a)\cdot e^{-ct}] + p\cdot t$. The parameters in this solution are as follows: n, order of nucleation; X_0, initial excess G-actin concentration = $A_0 - CC$; $a^{2/n}$, fraction of G-actin that polymerizes independently of synapsin I; c, $A_0^{n/2}\cdot a\cdot k$ (s^{-1}); k, G-actin/synapsin I association rate constant ($M^{-2/n}\ s^{-1}$); p, rate constant (s^{-1}) related to nucleation and elongation rate constants, K_n and K^+, and to the final concentration of filaments, F, by the following equations.

$$p = (n/2)\cdot K^+\cdot F_\infty \qquad (A14)$$

$$p^2 = (n/2)\cdot(A_0 - CC)^n\cdot a^2\cdot K_n\cdot K^+ \qquad (A15)$$

It is appropriate to point out that: (i) without synapsin I, from Equation 5 under the "Theory" section, we have the same definitions of the rate constant p, simply considering that, in that case, $a \equiv 1$; (ii) p, the analytical rate constant of the process, increases with the nth power of $(A_0 - CC)$, for fixed nucleation rate constant, K_n, and in fact the initial concentration of actin determines the overall speed of the polymerization curve (the value of n can be estimated from the slope of a log – log plot of polymerization speed *versus* initial G-actin concentration); (iii) the final rate of elongation, proportional to $2p/n = K^+\cdot F_\infty$ is independent of a (*i.e.* if it is reduced with increasing concentrations of synapsin I, then p must decrease, and $K^+\cdot K_n$ will also decrease unless p/a remains constant). Experimentally, the final elongation rate was decreased by synapsin I, indicating that either the number of filaments is decreased or most of them have a low elongation rate constant. Since cytochalasin B binding data indicate that the number of filaments is increased by synapsin I (Benfenati *et al.*, 1992), K^+ must decrease. Moreover, the ratio $F_\infty/K_n = A_0^n\cdot a^2/p$ should not decrease (and it does not, as shown in Fig. 5, *lower panel*) unless synapsin I markedly inhibited spontaneous nucleation, and therefore p should decrease more than a^2 with increasing concentrations of synapsin I.

REFERENCES

Attri, A. K., Lewis, M. S., and Korn, E. D. (1991) *J. Biol. Chem.* **266,** 6815–6824

Bähler, M., and Greengard, P. (1987) *Nature* **326,** 704–707

Bähler, M., Benfenati, F., Valtorta, F., Czernik, A. J., and Greengard, P. (1989) *J. Cell Biol.* **108,** 1841–1849

Bähler, M., Benfenati, F., Valtorta, F., and Greengard, P. (1990) *Bioessays* **12,** 259–263

Benfenati, F., Bähler, M., Jahn, R., and Greengard, P. (1989) *J. Cell Biol.* **108,** 1863–1872

Benfenati, F., Valtorta, F., and Greengard, P. (1991) *Proc. Natl. Acad. Sci. U. S. A.* **88,** 575–579

Benfenati, F., Valtorta, F., Chieregatti, E., and Greengard, P. (1992) *Neuron,* in press

Carlier M.-F. (1991) *J. Biol. Chem.* **266,** 1–4

Cooper, J. A., and Pollard, T. D. (1985) *Biochemistry* **24,** 793–799

Cooper, J. A., Buhle, E. L., Jr., Walker, S. B., Tsong, T. Y., and Pollard, T. D. (1983a) *Biochemistry* **22,** 2193–2202

Cooper, J. A., Walker, S. B., and Pollard, T. D. (1983b) *J. Muscle Res. Cell Motil.* **4,** 253–262

De Camilli, P., Benfenati, F., Valtorta, F., and Greengard, P. (1990) *Annu. Rev. Cell Biol.* **6,** 433–460

Doi, Y., and Frieden, C. (1984) *J. Biol. Chem.* **259,** 11868–11875

Flanagan, M. D., and Lin, S. (1980) *J. Biol. Chem.* **255,** 835–838

Frieden, C. (1983) *Proc. Natl. Acad. Sci. U. S. A.* **80,** 6513–6517

Frieden, C. (1985) *Annu. Rev. Biophys. Biophys. Chem.* **14,** 189–210

Gaertner, A., Ruhnau, K., Schröer, E., Selve, N., Wanger, M., and Wegner, A. (1989) *J. Muscle Res. Cell Motil.* **10,** 1–9

Glenney, J. R., Kaulfus, P., and Weber, K. (1981) *Cell* **24,** 471–480

Grazi, E. (1985) *Biochem. Biophys. Res. Commun.* **128,** 1058–1063

Huttner, W. B., Schiebler, W., Greengard, P., and De Camilli, P. (1983) *J. Cell Biol.* **96,** 1374–1388

Isenberg, G., Aebi, U., and Pollard, T. D. (1980) *Nature* **288,** 455–459

Korn, E. D. (1982) *Physiol. Rev.* **62,** 672–737

Kouyama, T., and Mihashi, K. (1981) *Eur. J. Biochem.* **114,** 33–38

Oosawa, F., and Asakura, S. (1975) in *Thermodynamics of the Polymerization of Protein,* pp. 109–118, Academic Press, New York

Petrucci, T. C., and Morrow, J. (1987) *J. Cell Biol.* **105,** 1355–1363

Pollard, T. D., and Cooper, J. A. (1986) *Annu. Rev. Biochem.* **55,** 987–1035

Schiebler, W., Jahn, R., Doucet, J.-P., Rothlein, J., and Greengard, P. (1986) *J. Biol. Chem.* **261,** 8383–8390

Südhof, T. C., Czernik, A. J., Kao, H.-T., Takei, K., Johnston, P. A., Horiuchi, A., Wagner, M., Kanazir, S. D., Perin, M. S., De Camilli, P., and Greengard P. (1989) *Science* **245,** 1474–1480

Tobacman, L. S., and Korn, E. D. (1983) *J. Biol. Chem.* **258,** 3207–3214

Valtorta, F., Greengard, P., Fesce, R., Chieregatti, E., and Benfenati, F. (1992) *J. Biol. Chem.* **267,** 11281–11288

Vandekerchkove, J. (1989) *Curr. Opin. Cell Biol.* **1,** 15–22

Wegner, A. (1976) *J. Mol. Biol.* **108,** 139–150

Wegner, A., and Engel, J. (1975) *Biophys. Chem.* **3,** 215–225

Yin, H. L., Hartwig, J. H., Maruyama, K., and Stossel, T. P. (1981) *J. Biol. Chem.* **256,** 9693–9697